Dynamical studies of CsH_2AsO_4 using EPR lineshapes, ENDOR results and theoretical calculations

1991 J. Phys.: Condens. Matter 3 6635

(http://iopscience.iop.org/0953-8984/3/34/009)

J. Phys.: Condens. Matter 3 (1991) 6635–6647. Printed in the UK

Dynamical studies of CsH_2AsO_4 using EPR lineshapes, ENDOR results and theoretical calculations

P K Kahol†‡, D T Scoular† and N S Dalal§

† Department of Physics and ‡ National Institute of Aviation Research, Wichita State University, Wichita, KS 67208, USA

§ Chemistry Department, West Virginia University, Morgantown, WV 26506, USA

Received 10 August 1990, in final form 8 April 1991

Abstract. The EPR spectra of the AsO_4^{4-} centre in CsH_2AsO_4 are overwhelmed by inhomogeneous broadening due to superhyperfine (SHF) interactions predominantly with one caesium and two protons but with small contributions from many other nuclei. The temperature dependence of these spectra shows marked changes in the temperature range 250–320 K and thus far has not been explained. Using a model which involves SHF coupling of the AsO_4^{4-} centre with two caesiums, two close protons and two far protons we have performed calculations based on the modified Bloch equations to simulate the EPR spectra. The ENDOR of ^{133}Cs and ^1H was also performed to obtain the necessary ingredients for computer simulations. Motional correlation times for the fluctuations involving relative motions of ^{133}Cs, ^{75}As and ^1H nuclei have thus been obtained in the temperature range 260–320 K. The near equality of these motional times which bears strong similarity to the soft-mode motions but on a different time scale is suggested and discussed.

1. Introduction

In this paper we wish to report on the correlated fluctuations of the ^{133}Cs, ^{75}As and ^1H nuclei in γ-irradiated CsH_2AsO_4 (CDA), using AsO_4^{4-} as a paramagnetic probe, via EPR, ENDOR and computer simulations. Most of the reported dynamical work to date via EPR and ENDOR has only been done on the potassium-based KDP-type materials and has been essentially concerned with obtaining correlation times for the motion of protons and ^{75}As nuclei ([1, 2] and references therein). The motion of the heavy cation potassium, however, has not been amenable to EPR investigations, thus making it difficult to draw definitive conclusions about the nature of the coupled radical centre–lattice motions. This has been due to the fact that potassium superhyperfine (SHF) coupling ($A_c \simeq 4$ MHz) is much smaller than that for caesium (A_c (nearest) ≈ 42 MHz, A_c (next nearest) ≈ 9 MHz) [3]. A much larger SHF value compared with that for potassium overwhelms the EPR lineshape in CDA [4, 5] and thus provides us with a sensitive methodology for investigating the relative motions of various ions such as, for example, Cs–H_4AsO_4 and H_4–AsO_4. Such motions are of significant interest since they have been implicated in a wide area of theoretical and experimental physics ([1, 2, 6–9] and references therein).

It is neither our intention nor our objective to provide an interpretation of the observed EPR/ENDOR correlation times in KDP-type materials, especially in CDA, which,

0953-8984/91/346635+13$03.50

as here, are about two to three orders of magnitude larger than the relaxational soft-mode times involved in the critical dynamics of T_C [10]. A number of experimental and theoretical papers are referred to here for gaining deeper insight into the nature of fluctuations as probed by EPR and ENDOR [1, 2]. Instead the objective is to obtain motional correlation times for the fluctuations of the heavy cation ^{133}Cs, protons and ^{75}As from simulations of the EPR lineshapes using modified Block equations [11, 12] and ENDOR. The implications of these correlation times are then discussed.

2. Materials and methods

Single crystals of CsH_2AsO_4, usually of the parallelepiped shape with the largest dimension as the polar c-axis, were grown from slow evaporation of an equimolar aqueous solution of Cs_2CO_3 and As_2O_5. The Curie temperature T_C was found to be 144 ± 1 K. The crystals were then irradiated with γ-rays at room temperature to a dose of about 10 M rad.

The EPR and ENDOR experiments were done in the X-band (9.5 GHz) using a Bruker ER200D spectrometer at 100 kHz magnetic field modulation. Operation of the spectrometer, especially for ENDOR studies, was controlled by an ASPECT 2000 mini-computer. A self-tracking NMR gaussmeter (Bruker model ER035M) calibrated precise values of the magnetic field whilst a Hewlett–Packard frequency counter (5340A) was used to measure the microwave frequency. The temperature was varied using a Bruker (ER4111VT) digital temperature controller. Alignment of the crystals in the magnetic field ($H \parallel c, H \parallel a$ and $H \parallel x$ where $x = a + 45°$) especially for ENDOR experiments was achieved to better than half a degree by monitoring a certain proton line of the ENDOR spectrum for $H \parallel c$ and/or $H \parallel a$.

3. Experimental results and their interpretation

3.1. Temperature dependence of the EPR lines

The AsO_4^{4-} centre, due to the hyperfine coupling with the ^{75}As nucleus ($I = \frac{3}{2}$), gives rise to a set of four EPR transitions labelled according to the $m_I = -\frac{3}{2}$ to $+\frac{3}{2}$ nuclear states [13, 14]. At the X-band, the line at the lowest field corresponds to $m_I = 3/2$ and occurs around 1400 G, whereas the highest field line corresponding to $m_I = -3/2$ occurs around 4800 G.

Figure 1 shows EPR spectra in the temperature range 270–320 K for the AsO_4^{4-} centre for $m_I = -\frac{3}{2}$ and $H \parallel c$. Below 200 K the EPR lineshape consists of 'two inverted Gaussians' separated by a 'linear' region essentially with zero slope. As the temperature is increased, the two inverted Gaussian peaks move closer and the slope of the linear region decreases. Around 300 K the linear region smoothly joins the two inverted peaks and with further increase in temperature, 'structure' appears around the centre position of the EPR spectrum. Simulations of these spectra, also shown in figure 1, will be discussed in section 3.4. Since the simulations require accurate values of the SHF coupling for Cs, we present in figure 2 the SHF couplings for $H \parallel c, A_c$, deduced from the separation between the two peaks of the spectrum divided by eight [15]. The agreement between the EPR-deduced and ENDOR-obtained values for the SHF couplings in the overlapping temperature regime where both measurements were feasible is very satisfactory.

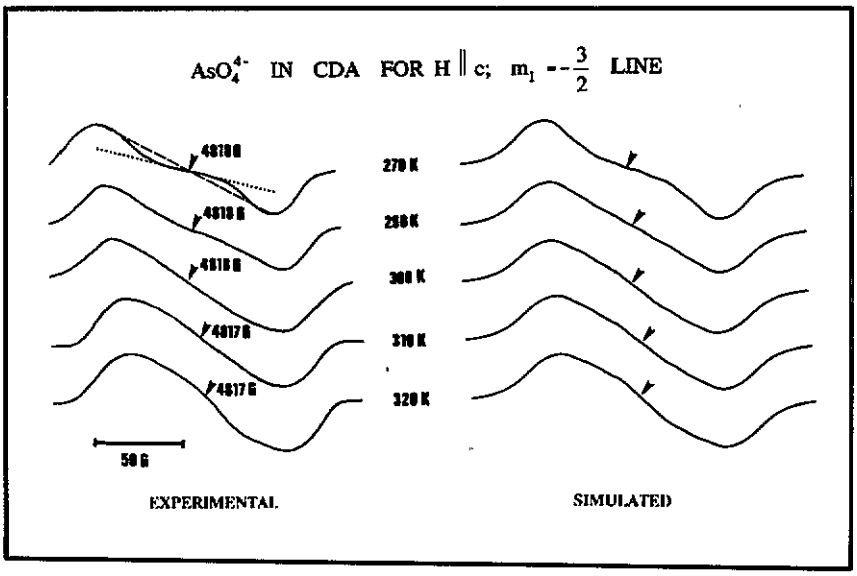

Figure 1. Experimental (left-hand side) and simulated (right-hand side) EPR spectra of the AsO_4^{4-} centre in CsH_2AsO_4 for $H \parallel c, m_I = -\frac{3}{2}$ in the temperature range 270–320 K. Arrows denote positions of the centre of the $m_I = -\frac{3}{2}$ line. For simulated spectra obtained using the model described in the text each line was given a width ($\approx 1/T_2$) of 11.3 G up to 270 K and 12.3 G above 270 K. This width includes all the interactions not considered explicitly in the model. Dotted and broken lines plotted in the spectrum at 270 K show the criterion, as explained in the text, to check quality of the simulated spectra.

Figure 3 shows typical spectra of the $m_I = \frac{3}{2}$ line for the field orientation $H \parallel x$ in the ab-plane for the temperature range 260–320 K. The spectrum is a simple superposition of two 'two inverted Gaussians' separated by ΔH, the doublet splitting or domain splitting. The variation of ΔH as a function of temperature is shown in figure 4(a) which exhibits a deviation from the linear behaviour from around 230 K upwards. As is to be discussed later, the values of ΔH lying on the straight line are used for simulating the EPR lineshapes. Figure 4(b) shows the values of the SHF couplings deduced from the peak-to-peak separations. These values will be used in simulating the EPR spectra of figure 3 and those shown in figure 5 for the situation $m_I = -\frac{3}{2}, H \parallel x$. Evolution of the lineshapes for $H \parallel x$ (figure 5) with an increase in temperature almost parallels that for the $H \parallel c$ case.

3.2. ENDOR of AsO_4^{4-} centre

In this section we briefly present the information needed for successful interpretation of the EPR spectra using the model to be discussed in the next section. First, it is crucial to identify SHF couplings due to the two caesiums lying on the c-axis. The angular variation of the various lines, identified as due to caesium nuclei, was therefore investigated in three mutually perpendicular crystallographic planes. Figure 6 shows the angular dependence of the ^{133}Cs ENDOR spectra in the ac- and ab-planes. Although we are not yet able to analyse the precise anisotropic character for the lines appearing below 3.5 MHz, it seems clear from the data shown in figure 6 that the SHF tensors for the two nearest caesiums are completely axial in the ab-plane. Second, it is necessary

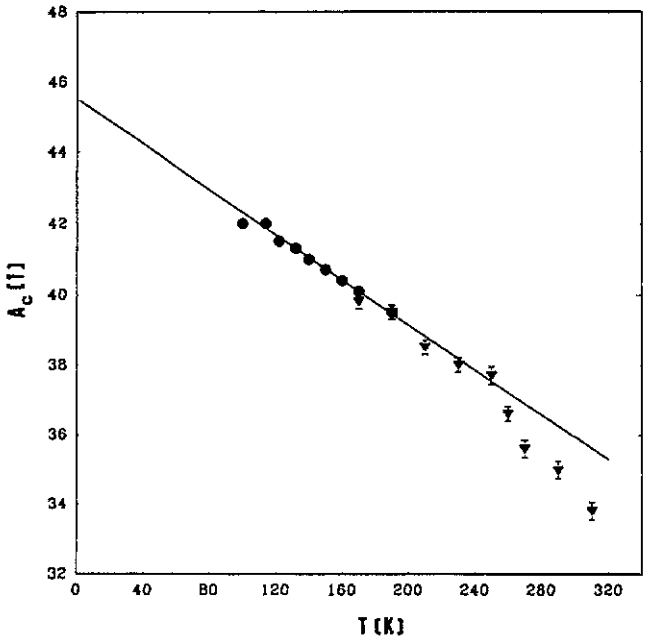

Figure 2. Temperature dependence of the experimental values of the SHF couplings for the nearest Cs as deduced from EPR data (full triangles) and directly obtained from ENDOR data (full circles).

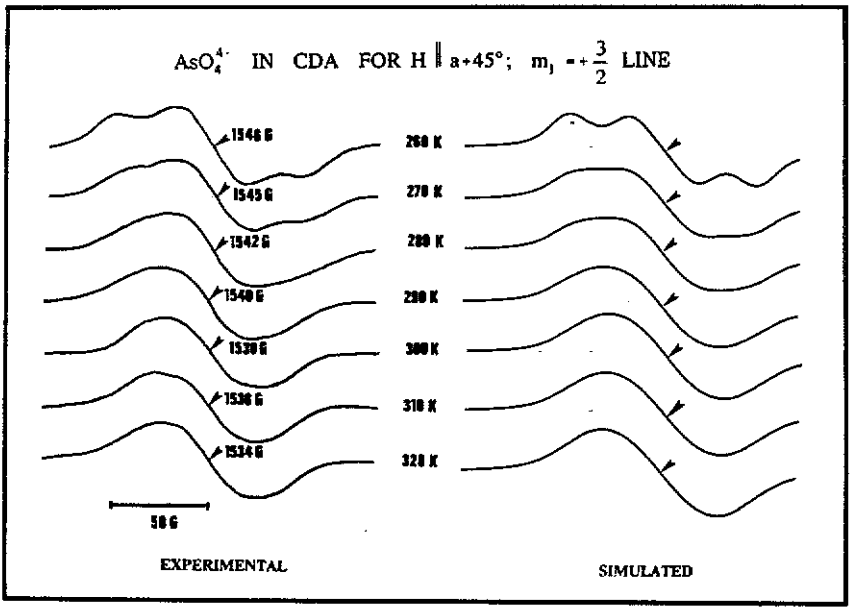

Figure 3. Experimental (left-hand side) and simulated (right-hand side) EPR spectra of the AsO_4^{4-} centre in CDA for $H \parallel x, m_I = \frac{3}{2}$ in the temperature range 260–320 K. The arrows on the simulated spectra correspond to the same values of the magnetic field as shown on the experimental spectra.

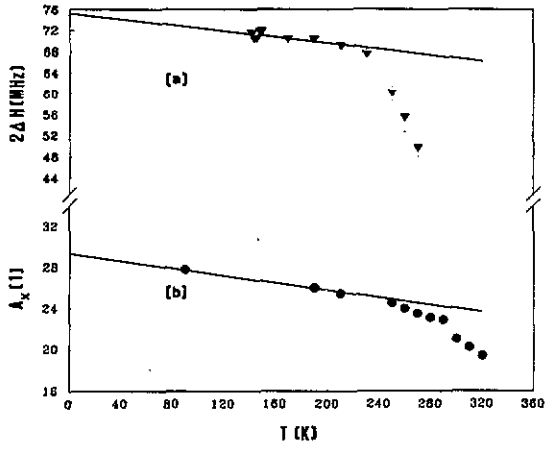

Figure 4. Temperature dependence of domain splitting, ΔH (full triangles, (a)) and Cs SHF coupling obtained from the EPR data (full circles, (b)) for AsO_4^{4-} in CDA.

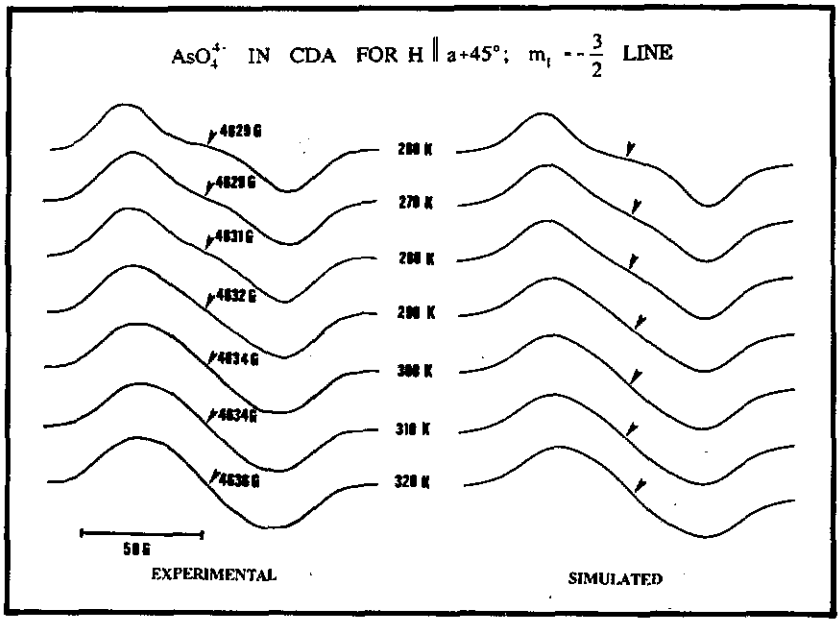

Figure 5. Experimental (left-hand side) and simulated (right-hand side) EPR spectra of AsO_4^{4-} in CDA for $H \parallel x, m = -\frac{3}{2}$ in the temperature range 260–320 K. The arrows on the simulated spectra correspond to the same values of the magnetic field as shown on the corresponding experimental ones.

to obtain a quantitative behaviour of the temperature dependence of these two ^{133}Cs SHF couplings. Using previously described procedures [16], we thus calculated the SHF tensor component for $H \parallel c$ up to $T = 210$ K. The results for the nearest caesium, shown on the same plot as the corresponding EPR-deduced SHF data (figure 2), show good agreement with the values deduced empirically from the EPR lineshapes. This is important since ENDOR signals could not be detected in the temperature range where the EPR spectra exhibit profound changes. The SHF coupling of the second nearest

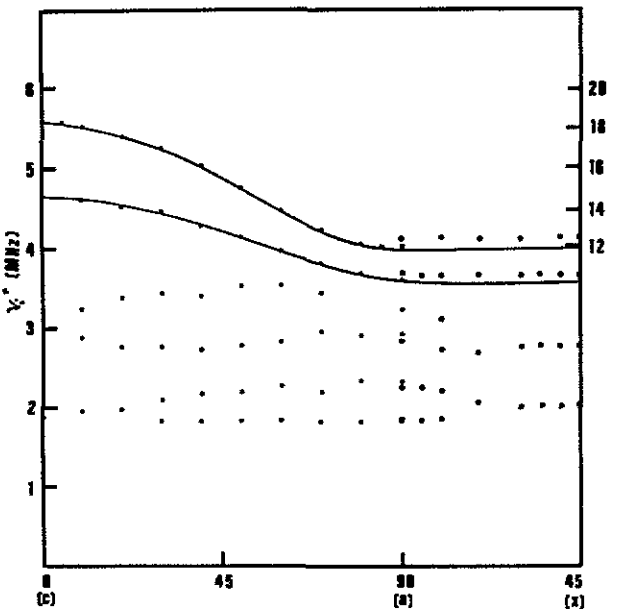

Figure 6. Angular dependence of ^{133}Cs ENDOR signals for the AsO_4^{4-} centre in CDA at 124 K. Slight mismatch at $H \parallel a$ is probably due to slight misorientation of the crystal. The scale shown on the right-hand side is for the nearest caesium atom (top curve).

caesium, however, shows no temperature dependence within experimental errors.

3.3. Theoretical model

The model used in the present simulations is based upon a spin-$\frac{1}{2}$ centre coupled to two non-equivalent, axial caesiums ($I = \frac{7}{2}$), two equivalent near protons ($I = \frac{1}{2}$) and two equivalent far protons ($I = \frac{1}{2}$). In the calculations both the equivalent pairs of near and far protons have been treated as near and far 'spin-1' nuclei but exhibiting 1:2:1 triplet patterns. The stick spectrum corresponding to this situation is schematically shown in figure 7 where m_{I1} and m_{I2} denote caesium spin quantum numbers, and m_{I3} and m_{I4} denote $I = 1$ spin quantum numbers. Each of the eight caesium lines corresponding to m_{I1} with separation $A(1)$ is split into eight by the second caesium SHF interaction $A(2)$. These lines are further split by 'spin-1' SHF interactions $A(3)$ and $A(4)$, with the resulting stick lines represented as $(m_{I1}, m_{I2}, m_{I3}, m_{I4})$. Each of these 576 lines denotes a particular set of quantum numbers in the representation $(m_{I1}, m_{I2}, m_{I3}, m_{I4})$.

Time-dependent effects are then included in this model assuming 'out-of-phase' modulations of the caesium and proton SHF interactions effected by 'two-site' (A↔B) motions of these nuclei. The motion of the protons between the two positions of the O–H...O double minimum potential well has already been shown by Blinc *et al* [17] in their pioneering work in KDP/KDA and related isomorphic potassium-based materials. In this paper we are implying possible motion of the heavy nucleus Cs in a double minimum potential well. Let us denote by τ_{Cs}, τ_H and τ_{As} the motional correlation times for the caesium, proton and arsenic nuclei, respectively. In the 'rigid-limit' regime, the time scale of the modulation of the SHF interactions is much slower than

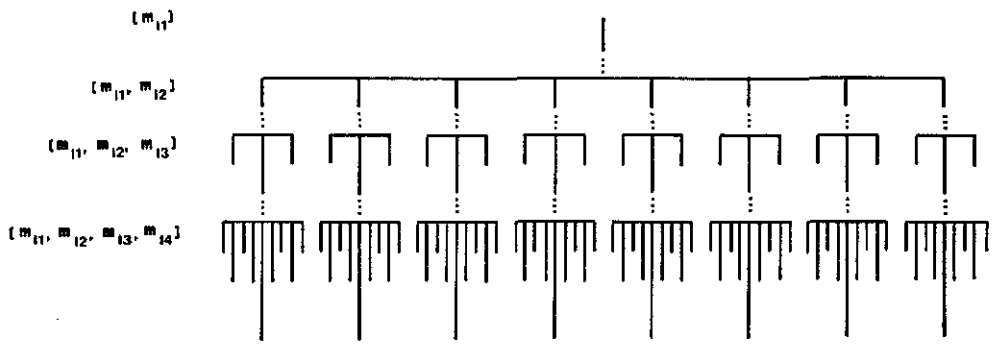

Figure 7. Schematic representation $(m_{I1}, m_{I2}, m_{I3}, m_{I4})$ of the spectrum, in the slow motional limit, of the AsO_4^{4-} radical coupled to two caesiums, one pair of two equivalent, near protons (considered as a 'spin-1' entity) and one pair of two equivalent, far protons (also considered as a 'spin-1' entity) for a fixed value of m_{I1}.

the experimental time scale, and thus the experimental spectrum can be reproduced from the stick spectrum giving each line a width representing life-time effects, residual spin/spin interactions and other line-broadening effects. The motional correlation times for this situation are typically larger than 10^{-7} s which is the upper limit of the EPR time scale. With an increase in temperature, the motional times become comparable with the EPR time scale and consequently the EPR lineshape shows marked changes. This is included in the model by exchanging the positions of the appropriate stick spectrum lines using modified Bloch equations. Situations of the following type, encountered in the simulation process, are dealt with as follows.

(i) Two lines with quantum numbers $(m_{I1}, m_{I2}, m_{I3}, m_{I4})$ and $(m'_{I1}, m'_{I2}, m'_{I3}, m'_{I4})$ exchange with the correlation time τ_{Cs} provided $m_{I3} = m'_{I3}, m_{I4} = m'_{I4}, m_{I1} = m'_{I2}$ and $m_{I2} = m'_{I1}$.

(ii) Lines exchange with the correlation time τ_H provided $m_{I1} = m'_{I1}, m_{I2} = m'_{I2}, m_{I3} = m'_{I4}$ and $m_{I4} = m'_{I3}$.

(iii) Lines are assumed to exchange with the correlation time given by the relation $1/\tau' = 1/\tau_{Cs} + 1/\tau_H$ if $m_{I1} = m'_{I2}, m_{I2} = m'_{I1}, m_{I3} = m'_{I4}$ and $m_{I4} = m'_{I3}$.

Line positions in angular frequency units are obtained in this way for the exchanging lines, and for each set of lines the derivative of the real part of the following well known formula [11] is used for obtaining the resultant ESR lineshape:

$$\nu = \frac{(1 + \tau/T_2)P + QR}{P^2 + R^2} \tag{1}$$

where

$$P = \tau\left[\left(\frac{1}{T_2}\right)^2 - (\Delta\omega)^2 + \frac{1}{4}(\delta\omega)^2\right] \tag{2}$$

$$Q = \tau\Delta\omega \tag{3}$$

$$R = \left(1 + \frac{2\tau}{T_2}\right)\Delta\omega \tag{4}$$

$$\Delta\omega = \tfrac{1}{2}(\omega_A + \omega_B) - \omega \tag{5}$$

$$\delta\omega = \omega_A - \omega_B. \tag{6}$$

In these equations, ω_A and ω_B denote the angular positions of the lines corresponding to sites A and B, respectively, T_2 is related to the linewidth, $\tau = \tau_A\tau_B/\tau_A + \tau_B$ and the population factors of the nuclei at the two sites are equal ($P_A = P_B$). τ in this analysis can be either τ_{Cs} or τ_H or their combination depending upon the spin quantum numbers of the lines to be exchanged. The resultant ESR spectrum is finally obtained by summing such individual spectra from all the corresponding pairs of stick spectrum lines.

3.4. Simulations of EPR spectra

The calculation of the EPR spectra using the model described in the preceding section requires knowledge of the SHF couplings for ^{133}Cs and protons corresponding to the two sites A and B, correlation times τ_{Cs}, τ_H and τ_{As}, and the parameter $(1/T_2)$ related to the width of each component line in the spectrum. As explained later, the SHF couplings for ^{133}Cs at various temperatures were obtained from the combined EPR and ENDOR data, whilst for protons they were taken from the published literature [1]. τ_{Cs}, τ_H and τ_{As} are treated as free parameters and independently varied in the range 10^{-6}–10^{-10} s. An optimum value of $(1/T_2)$ is chosen so as to 'smooth out' sharp structure at low temperatures. The width of the rising part of the upright peak in the experimental spectrum increases slightly ($\sim 10\%$) from $T = 90$ to $T = 320$ K. We have taken this variation into account through $(1/T_2)$ although its effect on the overall spectrum is only small. The results calculated for each of the three cases mentioned in section 3.1 are separately discussed in the following. It is to be noted that the EPR spectra for various orientations of the magnetic field at a given temperature must involve the same set of values for τ_{Cs}, τ_H and τ_{As}; undoubtedly the appropriate SHF couplings have to be used. Although this helps find a 'unique' set of correlation times for various nuclei, we also use the following criterion to check the overall reproducibility of the spectra. The ratio of the two slopes, one from the linear region and the other from the line connecting the two peaks, is obtained for each calculated spectrum and compared with that from the corresponding experimental spectrum. This is shown in figure 1 for the calculated spectrum at $T = 270$ K.

3.4.1. $H \parallel c, m_I = -\frac{3}{2}$ line. As shown in figure 2, SHF couplings $A_c(1)$ for the nearest caesium decrease almost linearly with increase in temperature up to around 240 K above which motional exchange effects lead to significant deviation from the linear behaviour. Assuming the slow decrease to be due to lattice expansion, values for $A_c(1)$ lying on the straight line above approximately 240 K should thus be used in the calculations; the exchange process lowers these values to the experimentally observed ones. The SHF couplings of the next-nearest caesium, $A_c(2)$, are not obtainable from EPR data and we make use of the limited ENDOR data. We thus treat $A_c(2)$ as temperature independent in our calculations with the expectation that its temperature dependence, if any, will not have any appreciable effect on the EPR simulations. $A_c(3)$ and $A_c(4)$, SHF couplings for protons, have been taken from our earlier paper [5]. The value of $(1/T_2)$ up to $T = 270$ K is taken to be 11.3 G whilst for $T > 270$ K it is around 12.3 G.

Having fixed the SHF couplings and $(1/T_2)$ at a given temperature, dependence of the EPR lineshapes on τ_{Cs} and τ_H was investigated. Whilst we will explicitly show this effect for $H \parallel x$ $m = -\frac{3}{2}$ line, we note that the set with $\tau_{Cs} \approx \tau_H$ yields spectra closest to the experimental ones. The overall agreement between the simulated (figure 1) and experimental spectra is considered as fairly satisfactory.

3.4.2. $H \parallel x, m_I = \frac{3}{2}$. Since for this situation we are dealing with an individual line out of the four lines of the AsO_4^{4-} quartet, exchange effects between the two differently oriented domains can be investigated considering two sets of lines represented as $(m_0, m_{I1}, m_{I2}, m_{I3}, m_{I4})$ and $(-m_0, m_{I1}, m_{I2}, m_{I3}, m_{I4})$ separated by a ΔH. m_0 is an additional quantum number with a fixed arbitrary value. The total number of lines for this situation thus becomes $2(2I_1 + 1)(2I_2 + 1)(2I_3 + 1)(2I_4 + 1) = 1152$. Motional exchange between the lines within the multiplets $(m_0, m_{I1}, m_{I2}, m_{I3}, m_{I4})$ and $(-m_0, m_{I1}, m_{I2}, m_{I3}, m_{I4})$ is the same as discussed in section 3.4, but for line exchange between these multiplets we have resorted to the following approximations. Let us denote the two lines by the quantum numbers $(m_0, m_{I1}, m_{I2}, m_{I3}, m_{I4})$ and $(-m_{0'}, m'_{I1}, m'_{I2}, m'_{I3}, m'_{I4})$. These lines will exchange with time τ_{As} if $m_{I1} = m'_{I1}, m_{I2} = m'_{I2}, m_{I3} = m'_{I3}, m_{I4} = m'_{I4}$; with time given by $1/\tau = 1/\tau_{Cs} + 1/\tau_{As}$ if $m_{I1} = m'_{I2}, m_{I2} = m'_{I1}, m_{I3} = m'_{I3}, m_{I4} = m'_{I4}$; with time given by $1/\tau = 1/\tau_H + 1/\tau_{As}$ if $m_{I1} = m'_{I1}, m_{I2} = m'_{I2}, m_{I3} = m'_{I4}, m_{I4} = m'_{I3}$; and with time $1/\tau = 1/\tau_{As} + 1/\tau_H + 1/\tau_{Cs}$ if $m_{I1} = m'_{I2}, m_{I2} = m'_{I1}, m_{I3} = m'_{I4}, m_{I4} = m'_{I3}$.

The values of ΔH lying on the straight line (figure 4(*a*)) have been used in the calculations of the EPR spectra shown on the right-hand side of figure 3 at various temperatures. The hyperfine couplings $A_x(1)$ to be used in the simulations were obtained from the EPR spectra in the same way as for the $H \parallel c$ orientation which are also shown in figure 4. Assuming that the Cs hyperfine tensor is axial, values of $A_x(2)$ (equal to $A_a(2)$) are obtained using the approximate relation

$$A^2_{eff}(2) = A^2_c(2)\cos^2\theta + A^2_a(2)\sin^2\theta \tag{7}$$

where $A_{eff}(2)$ is the observed experimental value of the effective SHF coupling as a function of θ, the angle between the *c*-axis and the orientation of the magnetic field in the *ac*-plane. From the angular dependence of the ENDOR line for the second-nearest Cs, $A_{eff}(2)$ is noted for three orientations namely 10°, 20° and 30° and then equation (7) is used, along with $A_c(2) = 3.27$ MHz as obtained from ENDOR, to obtain a mean value of $A_x(2)$ which comes out to be equal to 2.31 MHz. As $A_c(2)$ is independent of temperature, $A_x(2)$ is also treated as independent of temperature for model calculations. The tensor for the protons is, however, not axial and thus we must transform the proton tensor into a new coordinate system where x happens to be one of the axes. Using the values of the tensors for near and far protons given by Dalal [1] for KDA at 4.2 K, and arguing that these values are also appropriate for protons in CDA, we obtain the following values for the SHF couplings: $A_x(3) = -14.25$ MHz and $A_x(4) = -3.4$ MHz. Based upon the increase in the width of the rising part of the positive peak, $(1/T_2)$ has been varied from 10.4 G at 270 K to 11.1 G at 320 K.

The results of computer simulations using these inputs are shown in figure 3 and show satisfactory agreement with the experimental data. Here, at each temperature the corresponding correlation times $\tau_{Cs} \approx \tau_H$ obtained from the simulations of EPR spectra in figure 1 were used and τ_{As} was varied. It turns out that τ_{As} is also equal to $\tau_{Cs} \approx \tau_H$ within the discrimination allowed by these simulations.

3.4.3. $H \parallel x$ *and* $m_I = -\frac{3}{2}$. The doublet splitting ΔH is nearly zero for this case, and therefore the method of calculation is identical to that for the $H \parallel c$ case discussed in section 3.4.1. The procedure to obtain $A_x(1), A_x(2), A_x(3)$ and $A_x(4)$ has also been discussed in the previous section. The same values of τ_{Cs} and τ_H as those obtained in earlier cases are used in the calculations as a function of temperature. The EPR

spectra simulated in this way are presented in figure 5 which again shows satisfactory agreement with the corresponding experimental spectra.

We have also chosen this orientation to illustrate the effect of changing the correlation times τ_{Cs} and τ_H on the overall quality of the calculated spectra. This is shown in figure 8 at 270 K. The experimental spectrum at this temperature is labelled E which corresponds to the motional times $\tau_{Cs} = \tau_H = 3 \times 10^{-8}$ s. The spectra A–D show the effect of keeping τ_H fixed at 3×10^{-8} s and using the following values of $\tau_{Cs} = 3 \times 10^{-7}$ s (spectrum A), 3×10^{-8} s (spectrum B), 3×10^{-9} s (spectrum C) and 3×10^{-10} s (spectrum D), whilst the spectra F–H show the effect of keeping τ_{Cs} fixed at 3×10^{-8} s and using the following values of τ_H: 3×10^{-8} s (spectrum F), 3×10^{-9} s (spectrum G), and 3×10^{-10} s (spectrum H). It is clear that discernible changes occur in the lineshapes of the calculated spectra if either of these two correlation times (in fact also τ_{As}) is varied.

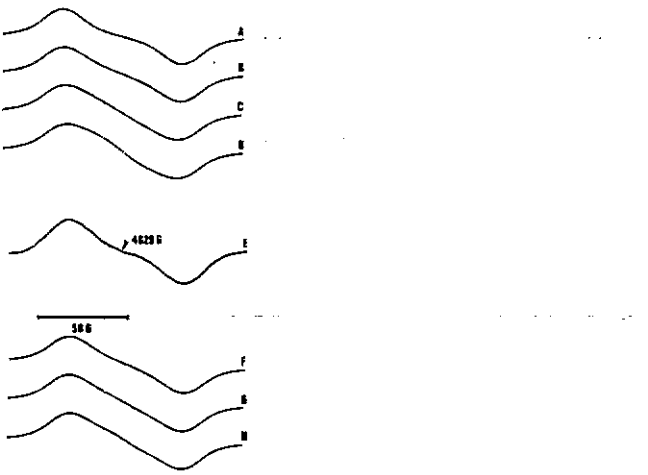

Figure 8. Dependence of the overall quality of the simulated spectra on varying caesium correlation times (A through D) and proton correlation times (F–H) at 270 K for $H \parallel x, m_I = -\frac{3}{2}$. Spectrum E is that obtained from experiments at 270 K, τ_H and τ_{Cs} in these calculations was kept fixed at 3×10^{-8} s.

4. Discussion

The important result to emerge from the model simulations is the near equality of the three motional correlation times $\tau_{Cs} \simeq \tau_H \simeq \tau_{As}$. The temperature dependence of these motional times in the temperature range 260–320 K is shown in figure 9. The data exhibit a linear behaviour and yield an activation energy of 0.46 eV. In other KDP-type lattices, the activation energies have ranged from about 0.20 eV in KDA to about 0.43 eV in deuterated ammonium dihydrogen arsenate [1].

Discernible changes due to motional process(es) in the EPR spectra start from around 250 K. The spectral coalescence temperature T^*, as determined from the coalescence of the doublet peaks arising from the two domains, is around 280 K. As expected the spectra change markedly around this temperature. Interestingly, very broad ^{133}Cs ENDOR signals are observable up to about 250 K, the same temperature

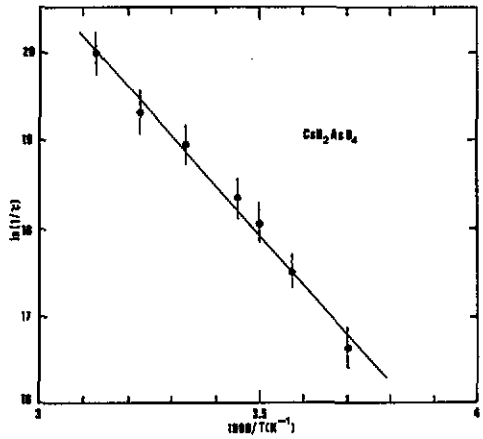

Figure 9. Arrhenius plot of the temperature dependence of the motional correlation times for AsO_4^{4-} in CDA obtained from simulations of the EPR spectra. Here $\tau_{Cs} \simeq \tau_{As} \simeq \tau_H$, and the activation energy is 0.46 ± 0.10 eV.

where EPR spectra undergo marked changes. Extrapolation of the behaviour shown in figure 9 toward lower temperatures yields correlation times, from T_C to $T_C + 50$ K, of the order of 10^{-6} s implying a too slow motion on the ENDOR time scale. On the other hand, our measurements detect significant linewidth changes in the ^{133}Cs ENDOR lines. We may therefore suggest two types of motional processes, one operative up to around 250 K and the other dominating above 250 K.

The fact that the plot of $\ln \tau$ against $1/T$ in figure 9 is linear and that no clear deviation of this linear behaviour is observed in the temperature range investigated, the applicability of the pseudo freeze-out model [18] seems to be questionable. According to this model, the activation energy should decrease with increase in temperature which clearly is not the case here. The existence of a single activation energy in the temperature range where EPR spectra exhibit significant changes is in keeping with similar conclusions arrived at recently by us from the ENDOR investigations of the proton lines of KDP [19–20]. In KDP/KDA, a linear behaviour of the data plotted as $\ln \tau$ against $1/T$ was obtained from both the ENDOR- and EPR-deduced values for τ [21].

The success in simulating the EPR lines for various orientations of the 'quartet' over the investigated temperature range via a simple model, which includes coupling of the AsO_4^{4-} centre with four protons and two off-centre caesiums and where the respective modulation of the ENDOR determined SHF couplings is out-of-phase, is quite convincing of the fact that one of the Cs^+ ions either below or above the AsO_4^{4-} centre is nearer to the centre. This might imply freezing-in of the 'soft-mode motions' as static structural displacements in the ferroelectric phase, proposed many years ago by Cochran [22] and Kobayashi [23] although the correlation times measured here are over two orders of magnitude longer than the time scale of even the slowest optical modes. In the soft-mode model for KDP, movement of the potassium and phosphorus (in antiphase) along the c-axis is coupled with the motions of hydrogens between their two sites which leads to approximately equal mean-square thermal amplitudes for the K- and P-atoms along the c-axis. In the revised soft-mode model [9], however, the mean-square thermal amplitude for the motion of caesium (or K) is zero but the

thermal amplitude for phosphorus (or As) is increased by nearly a factor of two. If our analogy to the soft-mode picture is taken a little further, the motional correlation rates for ^{133}Cs (shown in figure 9) would therefore denote the rates with which the two SHF couplings are modulated by the motion of the H_4AsO_4 unit between the two ferroelectric-phase configurations. As far as the present results are concerned, values obtained for τ_{Cs} denote the correlation times of the fluctuations in relative Cs–AsO_4 displacements. Nevertheless, the correlated nature of the fluctuations involving all the nuclei reflected through $\tau_{Cs} \simeq \tau_{As} \simeq \tau_H$ implies a motion analogous to the soft-mode type in spite of their different time scales.

The model described in this paper is simple, albeit physically realistic, and has provided a good description of the EPR lines for different orientations and over the entire investigated temperature range. It is, however, noted that we have had to include the presence of many smaller Cs SHF interactions indirectly into our model through the factor $(1/T_2)$. The magnitude of $(1/T_2)$ is of the order of 25 MHz which is somewhat large. It was found that if a third Cs SHF coupling of approximately 5 MHz is also considered and simple EPR calculations are performed for low temperatures (say, < 240 K), $(1/T_2)$ drops down to approximately 12 MHz. For our model calculations where only two Cs SHF couplings are explicitly considered a value of $(1/T_2)$ smaller than the one used introduces sharp 'structure' in the simulated spectrum. This is more so at lower temperatures than at higher temperatures, since relatively faster exchange at higher temperatures can 'wash-out' the structure somewhat. Choice of $(1/T_2)$ can, however, be difficult for cases where the interactions not explicitly considered in the model made a large broadening contribution or where the EPR spectrum showed more features. In either case, a smaller value of $(1/T_2)$ can be used and the simulated spectrum investigated for its 'envelope' lineshape.

5. Conclusions

Motional correlation times for the fluctuations of the various nuclei in CsH_2AsO_4 have been obtained from simulations of the EPR spectra of the AsO_4^{4-} centre through a heuristic model which includes multinuclear SHF couplings in a modified Bloch equations approach. Near equality of the correlation times has provided via EPR/ENDOR the 'first' evidence for the correlated nature of fluctuations involving the Cs, As and H nuclei. This has led us to draw a striking analogy with the soft-mode models. More theoretical and experimental work is certainly required for a better understanding of this apparent analogy. Proton and caesium ENDOR experiments through the phase transition temperature are already under way to understand further the nature of the implied analogy.

Acknowledgments

Thanks are due to Research Corporation for partial support of this work for PKK and to US Airforce for NSD.

References

[1] Dalal N S 1982 *Adv. Magn. Reson.* 10 119

[2] Müller K A 1987 *Ferroelectrics* **72** 273
[3] Dalal N S and Kahol P K 1989 *Solid State Commun.* **70** 623
[4] Sampaio J F, Ribeiro G M, Chaves A S and Gazzinelli R 1986b *J. Phys. C: Solid State Phys.* **19** 7269
[5] Kahol PK and Dalal N S 1988 *Solid State Commun.* **65** 823
[6] Blinc R and Zeks B 1982 *J. Phys. C: Solid State Phys.* **15** 4661
[7] Blinc R, Zeks B and Nelms R J 1983 *Phase Transitions* **3** 293
[8] Blinc R and Zeks B 1987 *Ferroelectrics* **72** 193
[9] Nelms R J 1987 *Ferroelectrics* **71** 87
[10] Blinc R and Zeks B 1974 *Soft Modes in Ferroelectrics and Antiferroelectrics* (Amsterdam: North-Holland) ch 7
[11] Gutowsky H S and Holm C H 1956 *J. Chem. Phys.* **25** 1228
[12] Wertz J E and Bolton J R 1986 *Electron Spin Resonance* (London: Chapman and Hall) ch 9
[13] Dalal N S, Dickinson J R and McDowell C A 1972b *J. Chem. Phys.* **57** 4254
[14] Lamotte B, Gaillard J and Constantinescu J 1972 *J. Chem. Phys.* **57** 3319
[15] Sampaio J F, Ribeiro G M, Rogueira R A and Chaves A S 1986a *Solid State Commun.* **57** 905
[16] Coope J A R, Dalal N S, McDowell C A and Srinivasan R 1972 *Mol. Phys.* **24** 403
[17] Blinc R, Cevc P and Cevc G 1979 *J. Chem. Phys.* **70** 153
[18] Ribeiro G M, Gonzaga L V, Chaves A S, Gazzinelli R, Blinc R, Cevc P, Prevlovsek P and Silkin N I 1982 *Phys. Rev.* B **25** 311
[19] Kahol P K and Dalal N S 1989 *Bull. Am. Phys. Soc.* **34** 934
[20] Dalal N S and Rakvin B 1989 *J. Chem. Phys.* **90** 5262
[21] Rakvin B, Kahol P K and Dalal N S 1989 *Mol. Phys.* **68** 1185
[22] Cochran W 1961 *Adv. Phys.* **10** 401
[23] Kobayashi K K 1968 *J. Phys. Soc. Japan* **24** 497